JOURNAL OF MATERIALS SCIENCE 20 (1985) 941–946

Changes in crystallinity and thermal effects in ground vaterite

C. BARRIGA, J. MORALES, J. L. TIRADO
Departamento de Química Inorgánica, Facultad de Ciencias, Universidad de Córdoba, Spain

The fractional conversion of vaterite into calcite promoted by grinding and its influence on the thermal behaviour of the samples is studied. The occurrence of a complex exothermal effect in the DSC curves is ascribed to the recovery of crystallinity of calcite and vaterite, on the basis of X-ray line profile analysis.

1. Introduction

The interest in the study of the mechanochemical processes is indicated by the large amount of work on this field that has been reported in recent years. Much of this work concerns alkaline earth carbonates. Vaterite, which is the least dense crystalline polymorph of calcium carbonate, may be transformed into calcite by thermal treatment or by prolonged grinding. The phase transition promoted at about 560° C has been studied using thermodynamic [1] and kinetic [2] data. On the other hand, the conversion of vaterite into calcite by mechanical treatment was first pointed out by Gammage and Glasson [3]. Northwood and Lewis [4] studied this process in detail, as well as the evolution of microstrains in ground vaterite. In a more recent publication, Gammage and Glasson [5] have emphasized the mechanochemical process, although additional data were not reported.

In this paper, the evolution of the thermal behaviour of ground vaterite, related to the sequences of crystallite size and microstrains in both ground vaterite and derived calcite, is discussed.

2. Experimental details

Synthetic vaterite was obtained as described by Rao [2]. The X-ray diffraction patterns of this sample reveal a high purity phase, calcite or aragonite being absent.

Grinding was performed in a Fritsch ME 030177 planetary mill, equipped with a cylindric agate mortar, 80 cm^3 capacity, and three balls, 10 mm diameter, of the same material. Starting with a charge of 10 g and after 7 h continuous grinding, portions of 0.5 g were withdrawn after each 120 min until a period of 50 h had elapsed.

Differential scanning calorimetry (DSC) was carried out using a Mettler TA 3000 apparatus. The DSC curves were obtained in a static air atmosphere at a heating rate of 6° C min^{-1}. Sample weights were about 25 mg. The integration of the peaks was performed by a Mettler TA processor unit.

Nitrogen adsorption isotherms were determined in a Pyrex high-vacuum apparatus. Pressures were read on a digital manometer Balzers APR-010 to within an accuracy of 0.1 mbar. The specific surface area was calculated using the BET method [6].

Scanning electron micrographs were obtained from a Phillips SEM 501B. Samples were dispersed by ultrasound in an acetone medium, settled on nickel holders and covered with an electrodeposited gold film.

X-ray diffraction patterns were recorded using a Phillips PW 1130 diffractometer, using Co$K\alpha$ radiation and an iron filter. X-ray diffraction line profiles were recorded by continuous scan at 0.125° min^{-1} and the intensities were read every 0.025° 2θ. Line profile analysis was carried out in the (1 0 4) reflection of calcite and the (1 1 0) and (1 1 1) lines of vaterite. A highly crystalline, natural sample of calcite provided the instrumental profile of the (1 0 4) line. This profile was also used in the analysis of the vaterite lines, as it was not

0022–2461/85 $03.00 + .12

possible to obtain an adequately crystalline vaterite sample. The centroid position and background level were corrected by means of a computer program based on that of Edwards and Toman [7].

The determination of crystallite size and microstrains was developed by the variance method. First, the slope and intercept of the variance–range curves of the h and g profiles corrected for truncation [8] were used to compute the slope (k_f) and intercept (Wo_f) of the profiles. Slopes were simply substracted while the intercepts were corrected for the non-additivity error [9]. The values of k_f and Wo_f were used in the calculation of crystallite size (ϵ_k) and the variance of the lattice strain distribution ($\langle e^2 \rangle$) by means of the equation of Langford and Wilson [10], in which:

$$k_f = \lambda/(\pi^2 \epsilon_k \cos\theta)$$
$$Wo_f = 4 \tan^2\theta \langle e^2 \rangle - \lambda^2/(4\pi^2 \epsilon_k^2 \cos^2\theta), \quad (1)$$

where λ is the radiation wavelength and θ the angle of the line centroid.

3. Results and discussion

Fig. 1 shows the X-ray diffraction patterns of several selected samples. First, it must be noted that the lines observed in the pattern of the original vaterite (0 h) correspond exclusively to this phase. As grinding time increases, the mechanical transformation of vaterite into calcite takes place, as can be observed in the diffractograms. However, this transformation is not completed, at least in 50 h, and a partial phase transition of calcite into aragonite is detected after 30 h. These effects disagree with the results of Gammage and Glasson [3], who found that after 25 h, calcite was the only detectable phase, while a more prolonged grinding converted most of the calcite into aragonite. At this point, it should be mentioned that the transformation of calcite into aragonite and vice versa, induced by grinding, has been widely studied [11] and in principle, should be independent of the origin of calcite. Thus, the divergence from the results of Gammage and Glasson [3] may be due to the different type of mill used in the mechanical treatment.

In addition to these phase transitions, the patterns in Fig. 1 show some variations in the broadening of the lines of calcite and vaterite. These changes should be reflected in crystallite size and/or microstrain variations. Before dealing

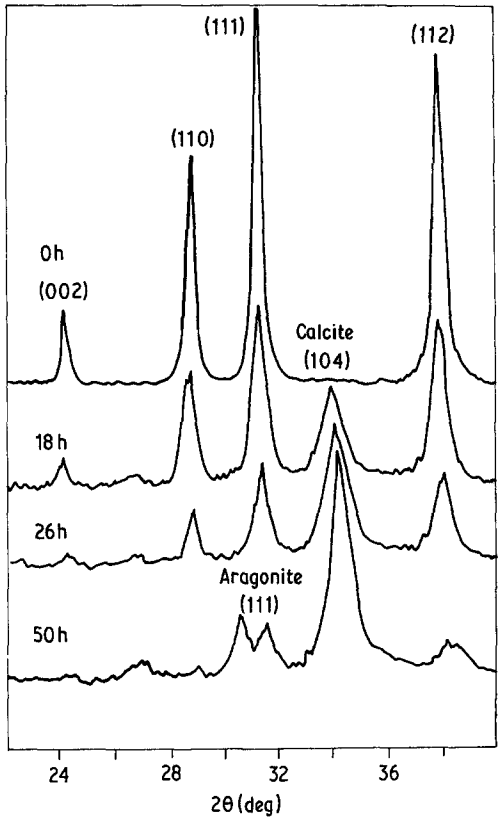

Figure 1 X-ray diffraction patterns of the original vaterite (0 h) and samples ground for 18, 26 and 50 h.

with these aspects, the evolution of particle size through grinding may be evaluated from a plot of BET surface against grinding time (Fig. 2), although the contribution of calcite and vaterite to the specific surface area of the samples cannot be separated. This plot shows an increase in

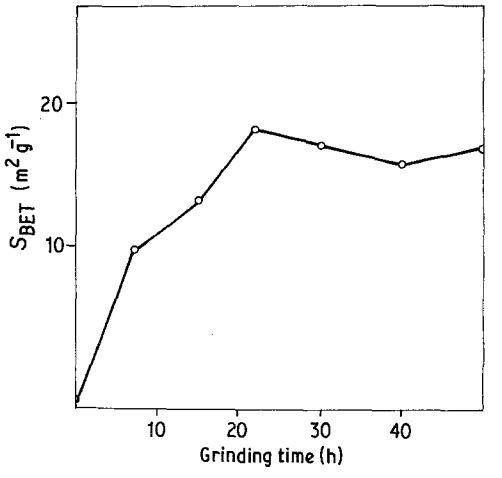

Figure 2 Plot of BET surface against grinding time.

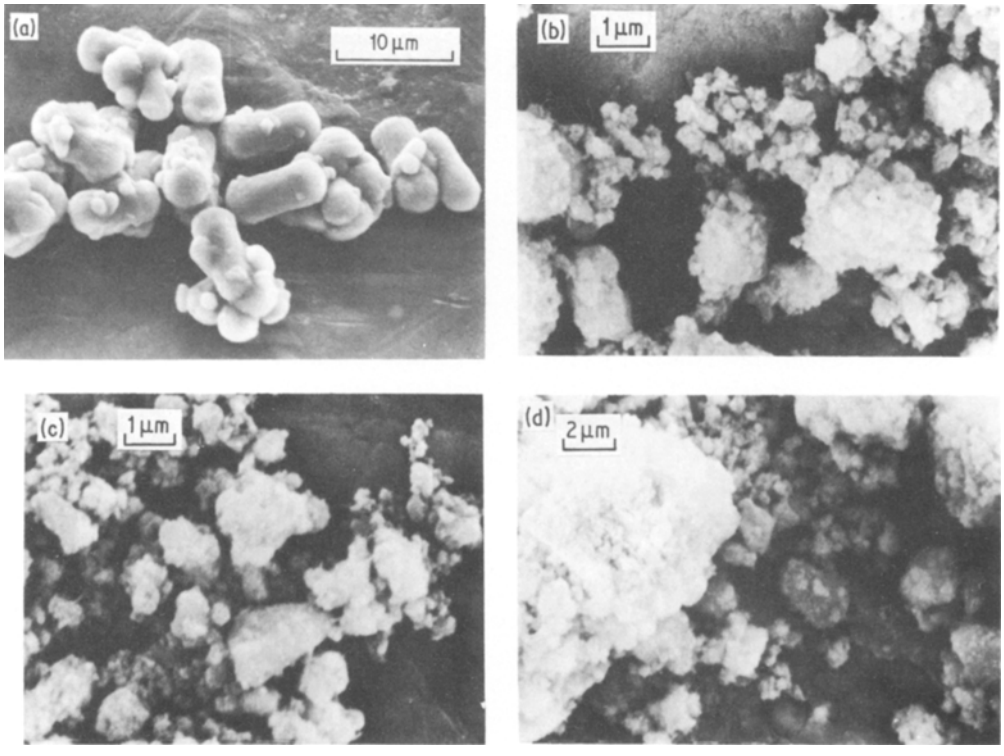

Figure 3 Scanning electron micrographs of several selected samples: (a) original vaterite; (b) 7 h; (c) 18 h; (d) 50 h.

specific surface at low grinding time, caused by the rupture of the original particles, while further grinding does not alter significantly the values of S_{BET}.

Fig. 3 shows the scanning electron micrographs of several samples. Unground vaterite presents a typical "peanut-like" shape (Fig. 3a). This shape is altered with grinding and smaller particles with lower sphericity are developed (Fig. 3b). The occurrence of these particles is connected with the rupture of vaterite crystals when the mechanical treatment is not sufficiently prolonged. With longer grinding times, the particles show a minimum in their size (between 18 and 24 h, Fig. 3c). Further milling is not accompanied by a decrease in particle size but a sintering process can be detected. At this time, calcite is already present (see Fig. 1, 18 h) but its particles cannot be recognized. After 30 h, some sharp-edged particles mixed with a more finitely divided powder are shown in the electron micrographs (Fig. 3d). These are different from the crystals previously described and may be identified as calcite crystals generated in the transformation of vaterite. This evolution is supported by the results of crystallite size determination.

Fig. 4 shows the DSC curves of the original

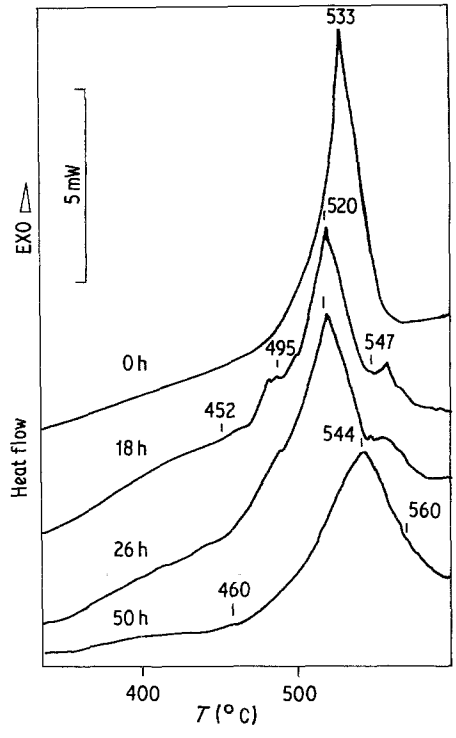

Figure 4 DSC traces of the original vaterite and samples ground for 18, 26 and 50 h.

vaterite sample and those corresponding to 18, 36 and 50 h grinding. For the unground vaterite, an exothermal effect placed at ca. 533° C is observed. This peak results from the thermal transformation of vaterite into calcite and occurs at a temperature slightly lower than that reported by Rao [2]. However, the effect is clearly exothermic, in contrast to the result reported by Davies *et al.* [12]. On increasing the grinding time, the shape of this peak shows a remarkable change. Besides a more pronounced broadening, two shoulders before and after the peak maximum are developed (see, for example, 18 h in Fig. 4). After 20 h, the lower temperature shoulder decreases in intensity until it becomes undetectable and the temperature of the peak maximum increases until it is near the position of the second shoulder. Some additional data may be obtained by plotting ΔH against grinding time (Fig. 5). It seems worthy to note from this plot that the variations in ΔH are small and fall within experimental error, even taking into account the progressive diminution in the vaterite content.

The presence of the above-mentioned shoulders and the constancy in integrated ΔH in the DSC curves must be explained in terms of the three main processes which can take place when ground vaterite is heated: phase transition of vaterite into calcite, recrystallization of calcite and recrystallization of vaterite. The following data are discussed on the basis of these assumptions.

Table I shows the results of the variance analysis of the selected line profiles. First, it should be noted that truncation errors ($\Delta k/k$) are within acceptable limits (3 to 9%), in correspondence with the values of the maximum range of scan, expressed in FWHM units (σ_2/FWHM). From the determination of crystallite size and microstrains in the (1 0 4) line of calcite, it seems that crystallinity in vaterite-derived calcite is small for all samples. However, a minimum in crystallite size appears between 15 and 20 h, while microstrains increase slightly on grinding. This result is in agreement with the loss of crystallinity originating from mechanical treatment of calcite [13]. On the other hand, the changes in crystallite size differ

TABLE I Results of the variance analysis of the lines of several selected samples of ground vaterite

h k l	σ_2/FWHM	FWHM	$\Delta k/k$	Wo_g	k_g			
1 0 4	4.26	3.27	3.5	−5.9	4.6	g profile		
h k l	σ_2/FWHM	FWHM	$\Delta k/k$	Wo_f	k_f	ϵ_k	$\langle e^2\rangle^{1/2}$	Grinding time (h)
1 1 0	4.41	6.10	7.9	−27.0	12.5	14.9	2.09	0
1 1 1	4.00	6.32	6.6	−5.2	9.2	20.6	2.21	
1 0 4	4.51	7.63	8.1	−65.7	20.8	9.3	3.08	
1 1 0	3.82	6.10	8.3	−62.8	17.6	14.5	1.80	7
1 1 1	3.86	6.65	7.0	−23.7	15.0	18.1	2.96	
1 0 4	3.88	11.12	8.6	−14.9	28.9	6.5	3.94	
1 1 0	4.06	7.19	6.2	−21.5	11.9	15.6	2.27	15
1 1 1	3.77	7.84	5.5	3.6	10.8	17.5	3.20	
1 0 4	3.82	12.43	7.8	−15.4	29.0	6.5	3.78	
1 1 0	3.82	7.63	5.5	−12.7	10.5	17.7	2.43	20
1 1 1	4.63	8.29	5.6	−31.7	17.3	10.9	3.63	
1 0 4	4.07	11.34	5.4	−37.0	18.8	10.0	3.62	
1 1 0	3.94	7.63	6.1	−16.6	12.6	14.8	2.92	26
1 1 1	3.95	8.94	9.5	−12.6	26.3	7.1	3.72	
1 0 4	4.05	11.56	5.16	−20.6	18.4	10.3	4.09	30
1 0 4	3.63	12.00	5.45	−0.8	17.9	10.6	4.55	40
1 0 4	4.14	12.65	5.18	−24.4	16.2	9.3	4.57	50

σ_2/FWHM : maximum range of scan (in FWHM units)
FWHM : full width at half maximum (rad × 10^3)
$\Delta k/k$: truncation error (%)
Wo_f : intercept of the variance–σ curves (rad^2 × 10^7)
k_f : slope of the variance–σ curves (rad × 10^4)
ϵ_k : crystallite size (nm)
$\langle e^2\rangle$: variance of the lattice strain distribution (× 10^3)

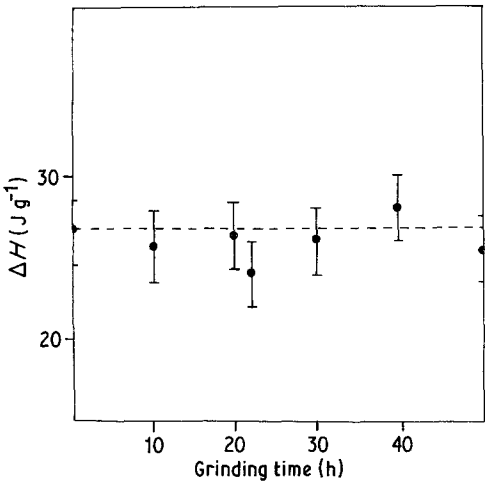

Figure 5 Plot of integrated ΔH against grinding time.

from previous studies on X-ray line broadening in plastically deformed calcite [14]. These changes are in correspondence with the sintering process obseved in Fig. 3.

On the other hand, the evolution of crystallite sizes and microstrains of vaterite (Table I) differs from that of calcite and depends on the line that is chosen in the variance analysis. In this way, crystallite size in the [1 1 1] direction decreases progressively while the changes are not so notable for the (1 1 0) line. The increase in microstrains is also less sharp in the latter direction. The changes in crystallite size for the (1 1 1) line show a significant discrepancy with the results of Northwood and Lewis [4], who find a constant intercept in the plots of β^{*2} against d^{*2} in ground vaterite. However, these authors use the (1 1 0), (1 1 1) and (1 1 2) lines of vaterite to obtain this plot. As these lines are not multiple-order reflections, they should not be included in the same sequence if the isotropy in crystallite size is not confirmed. In addition, the accuracy of a method which makes use of the integral breadths is dependent on a precise choice of background level, while this is automatically adjusted in the variance method.

The progressive loss of crystallinity in ground vaterite may shed new light on the thermal behaviour of these samples. As Turnbull [1] has pointed out, the values of ΔH increases when the crystallinity of vaterite is low. If we take into account that vaterite contents decrease as its transformation to calcite progresses, the lower crystallinity of vaterite may contribute to the constancy in ΔH for these samples.

In order to study the possibility that a recrystallization process could be involved in the complex thermal effect in the DSC curves of ground vaterite, several heated samples were prepared by interrupting the DSC measurements at various temperatures. Fig. 6 shows the X-ray diffraction patterns of these samples. When the sample ground for 18 h is heated to a temperature below the exothermal effect (Fig. 6b), no phase transition should be expected. However, a small change in the intensity and broadening of the lines is observed. On the other hand, once the exotherm is developed (Figs. 6c and d), vaterite transforms into calcite and the (1 0 4) lines are less broadened. In this way, the exotherm may be related to both effects, although it needs further confirmation by

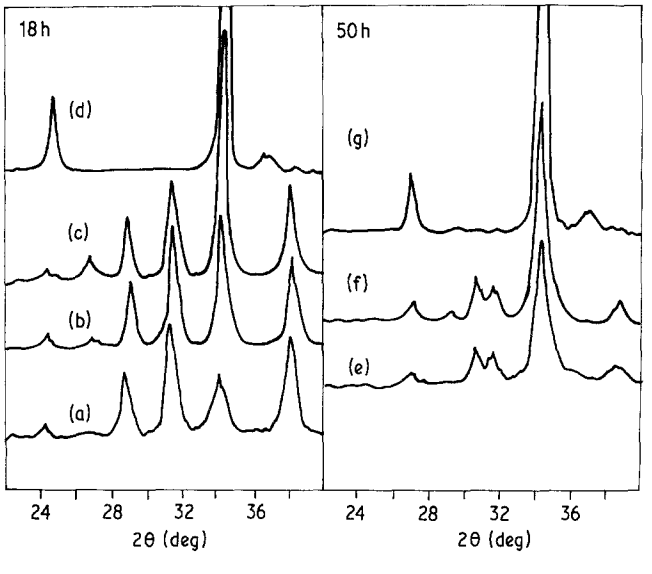

Figure 6 X-ray diffraction patterns of ground vaterite heated at different temperatures. 18 h sample: (a) 50° C, (b) 452° C, (c) 525° C, (d) 547° C; 50 h sample: (e) 50° C, (f) 460° C, (g) 560° C.

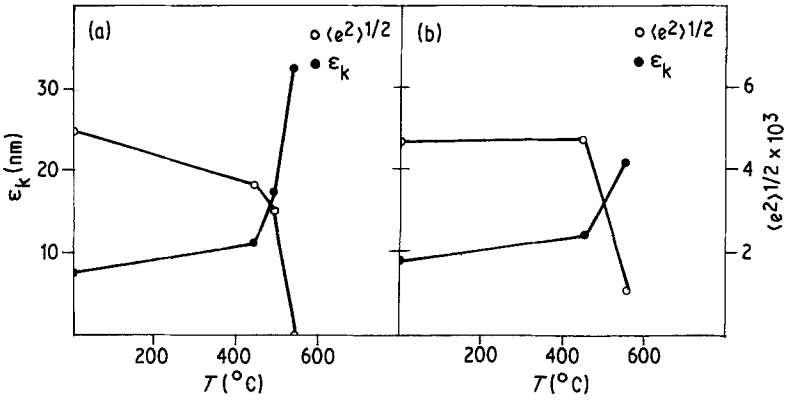

Figure 7 Plot of crystallite size and microstrains against temperature. (a) 18 h sample, (b) 50 h sample.

the application of the variance method. When the thermal evolution is followed for the 50 h ground sample, the main difference is the presence of aragonite (Figs. 6e and f), which disappears after the exothermal peak (Fig. 6g), giving additional complexity to the effect.

The application of the variance method to the diffraction lines of these heated samples yields to the values of crystallite size and microstrains in calcite which are plotted against temperature in Fig. 7. This plot shows a clear change in these parameters in the small temperature interval in which the exothermal peak develops. In particular, Fig. 7 shows that the recovery of crystallinity occurs in the final part of the exotherm. Gammage and Glasson [15] have shown that ground calcite recovers its crystallinity between 200 and 400° C, a lower temperature than that corresponding to calcite derived from ground vaterite.

Moreover, the process shown in Fig. 7 may have an influence on the thermal behaviour of the samples. Recently, it has been reported that the occurrence of an exothermal effect in the DSC curves of ground dolomite originated from a recrystallization process [16]. A similar explanation may be assumed for the high-temperature shoulder formed in the vicinity of the exothermic peak of the phase transition of vaterite into calcite. As the conversion promoted by grinding is more advanced (Fig. 7b), the recovery of crystallinity in calcite may be the main item responsible for the liberation of energy. This fact is supported by the displacement of the peak maximum to a temperature closer to 547° C in the DSC curve.

Acknowledgement

This work was carried out with the financial support of CAICYT (contract 0608/81).

References

1. A. G. TURNBULL, *Geochim. et Cosmochim. Acta* **37** (1973) 1596.
2. M. S. RAO, *Bull. Chem. Soc. Jpn* **46** (1973) 1414.
3. R. B. GAMMAGE and D. R. GLASSON, *Chem. Ind.* (1963) 1466.
4. D. O. NORTHWOOD and D. LEWIS, *Amer. Mineral.* **53** (1968) 2089.
5. R. B. GAMMAGE and D. R. GLASSON, *J. Colloid Interface Sci.* **55** (1976) 396.
6. S. BRUNAUER, P. H. EMMETT and E. TELLER, *J. Amer. Ceram. Soc.* **60** (1938) 309.
7. H. J. EDWARDS and K. TOMAN, *J. Appl. Cryst.* **4** (1971) 332.
8. J. I. LANGFORD, *ibid.* **15** (1982) 315.
9. A. J. C. WILSON, *ibid.* **3** (1970) 71.
10. J. I. LANGFORD and A. J. C. WILSON, in "Crystallography and Crystal Perfection", edited by G. N. Ramachardran (Academic Press, London, 1963) p. 207.
11. G. MARTINEZ, J. MORALES and G. MUNUERA, *J. Colloid Interface Sci.* **81** (1981) 500.
12. P. DAVIES, D. DOLLIMORE and G. R. HEAL, *J. Thermal. Anal.* **13** (1978) 473.
13. R. B. GAMMAGE, H. F. HOLMES, E. L. FULLER Jr and D. R. GLASSON, *J. Colloid Interface Sci.* **47** (1974) 350.
14. M. S. PATERSON, *Phil. Mag.* **4** (1959) 451.
15. R. B. GAMMAGE and D. R. GLASSON, "Colloid Interface Science", Vol. 5 (Academic Press, New York, (1976) p. 437.
16. J. MORALES and J. L. TIRADO. *Mat. Chem. Phys.* **10** (1984) 225.

Received 11 April
and accepted 10 May 1984